M. Briane

Three models of non periodic fibrous materials obtained by homogenization

THREE MODELS OF NON PERIODIC FIBROUS MATERIALS OBTAINED BY HOMOGENIZATION (*)

by M. BRIANE ([1])

Communicated by O. PIRONNEAU

Abstract. — *We describe here three models of fibrous materials in conduction (the results apply as well in elasticity). The fibers are not periodically arranged but their orientation varies continuously in the material. The human heart is an example of such a material. The models are obtained through the homogenization of the fibrous structure.*

Résumé. — *On présente ici trois modèles de matériaux fibrés dans le cas de la conduction (les résultats s'étendent au cas de l'élasticité). Les fibres ne forment pas un réseau périodique car leur orientation varie continûment dans le matériau, comme dans le cœur humain par exemple. Ces modèles sont obtenus par homogénéisation de la structure fibrée.*

1. INTRODUCTION

The cells of the human heart form fibers. Anatomic studies (*see* [Str]) have shown that cardiac fibers have preferential directions : they are nearly parallel to the cardiac wall and their orientation varies continuously from an angle γ_0 at the endocardium to $- \gamma_0$ at the epicardium.

Several biomechanicians (*see* [Pes], [Art], [Fsei] and [Cha]) have studied the mechanics of the cardiac muscle (especially the left ventricle) by modelling the heart as a material composed of fibers imbedded in a homogeneous medium. The stress tensor of their model can be written

$$\Sigma = \Sigma_m + T \quad \tau \otimes \tau$$

where Σ_m is the mediums tensor, T the fibers tension and τ the fibers direction.

(*) Manuscript received October 1992.
([1]) Laboratoire d'Analyse Numérique, Tour 55-65, Université Paris 6, 4 Place Jussieu, 75252 Paris Cedex 05.

Two defaults appear in this modelling :

— interaction between fibers and medium is neglected
— fibers are dimensionless.

The present work avoids the above defaults. It is based on the examination of a three dimensional geometry which exactly describes the fibrous structure. It models the mechanical behaviour of a fibrous material whose basic geometry is given by :

— fibers are cylinders of diameter ε
— fibers are perpendicular to the x_1-axis and make locally an angle $\gamma(x_1)$ with the x_2-axis, where γ is a given continuous function.

We shall describe the mechanical behaviour of such fibrous materials in conduction but results also apply in elasticity. Let A^1 be the fibers matrix and A^2 the medium matrix (where matrices A^k are symmetric and definite positive). The mechanical behaviour law of the fibrous material is then defined by the matrix-valued function

$$A^{\iota} = \chi^{\varepsilon} A^1 + (1 - \chi^{\varepsilon}) A^2 \tag{1.1}$$

where χ^{ε} is the characteristic function of the fibers.

The associated conduction problem is defined by :

$$\mathscr{P}(A^{\varepsilon}) \qquad \begin{cases} - \operatorname{div} A^{\varepsilon} \nabla u^{\varepsilon} = f & \text{in } \Omega \\ u^{\varepsilon} = 0 & \text{on } \partial\Omega . \end{cases}$$

where Ω is the open set of $\mathbf{R}^3$ where the problem is considered (e.g. the cardiac wall).

Conduction equation cannot be directly used if there are too many fibers in the material (like in the heart for example) i.e. when their radius ε is too small. We will thus use homogenization theory which consists in obtaining a limit problem $\mathscr{P}(A^0)$ where ε converges to 0 (*see* e.g. [Spa], [Mur], [B.L.P.] and [San]). In this theory, the matrix A^0 is determined independently of the right-hand side f by the following limits

$$\begin{aligned} u^{\varepsilon} &\xrightarrow{\text{weak}} u^0 \\ A^{\varepsilon} \nabla u^{\varepsilon} &\xrightarrow{\text{weak}} A^0 \nabla u^0 \end{aligned} \tag{1.2}$$

where the scalar function u^0 is the solution of the problem

$$\mathscr{P}(A^0) \qquad \begin{cases} - \operatorname{div} A^0 \nabla u^0 = f & \Omega \\ u^0 = 0 & \partial\Omega . \end{cases}$$

The matrix-valued function A^0 is the homogenized matrix of the composite material.

For example, *periodic* fibrous materials are classically modelized by homogenization as follows (*see* [B.L.P.], [San]) :

The matrix A^ε of the periodic fibrous material is defined by

$$A^\varepsilon(x) = A(x/\varepsilon) \text{ with } A(y) = \chi(y) A^1 + (1 - \chi(y)) A^2 \qquad (1.3)$$

where χ is Y-periodic here the $\mathbf{R}^2$ cube $Y = [-s/2 ; s/2]^2$ is the basic period of the material (see fig. 1).
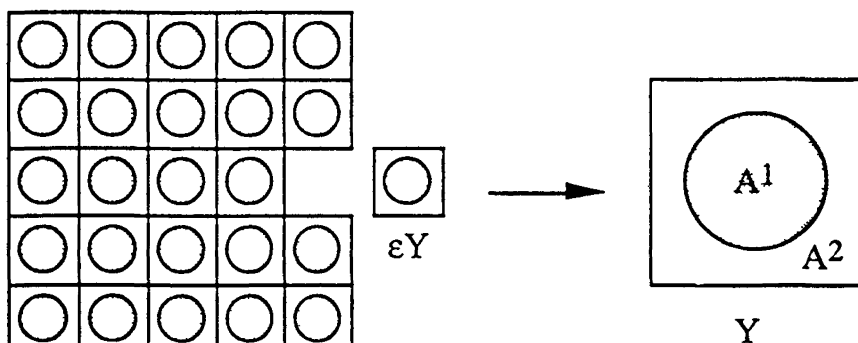

Figure 1.

It can then be proved that homogenized matrix-valued function A^0 is constant and defined by the formula (see [B.L.P.], [San]) :

$$A^0 \lambda = \frac{1}{|Y|} \int_Y [A(y) \lambda - A(y) \nabla \psi_\lambda(y)] \, dy \quad \forall \lambda \in \mathbf{R}^3 \qquad (1.4)$$

where function ψ_λ is the unique solution (up to an additive constant) of the differential equation

$$\begin{cases} \text{div } [A(y) \nabla \psi_\lambda(y)] = \text{div } [A(y) \lambda] & \text{in } \mathbf{R}^2 \\ \psi_\lambda \text{ } Y\text{-periodic} . \end{cases} \qquad (1.5)$$

In the present paper, we shall study three models of fibrous materials by defining three matrix-valued functions A^ε by formula (1.1). Of course characteristic function χ^ε will not be periodic. We shall then obtain by homogenization the corresponding homogenized matrices A^0. Each model will describe different modes of orientation of the fibers in the material.

The first model (studied in Chapter 2) is defined by the characteristic function χ^ε of the form

$$\chi^\varepsilon(x) = \chi(\rho(x)/\varepsilon) \quad \text{where} \quad \rho(x) = (x_1, \cos \gamma(x_1) x_3 - \sin \gamma(x_1) x_2) \qquad (1.6)$$

and the function χ is defined in (1.3).

The function ρ takes the same values along straight lines which are perpendicular to the x_1 axis and make an angle $\gamma(x_1)$ with the x_2-axis (*see* Section 2 1)

A homogenization result similar to formulas (1 4) and (1 5) is given in Section 2 2 and shows that the homogenized matrix $A^0(x)$ depends on the matrix-valued function

$$\nabla\rho(x) = \begin{pmatrix} 1 & 0 & 0 \\ -d(x) & -\sin\gamma(x_1) & \cos\gamma(x_1) \end{pmatrix},$$

$$d(x) = \gamma'(x_1)[\cos\gamma(x_1)\,x_2 + \sin\gamma(x_1)\,x_3] \tag{1 7}$$

But this model describes non cylindrical fibers because of the continuity of the function γ (*see* Section 2 3)

To obtain cylindrical fibers, we consider in Chapter 3 a second model which is stratified by layers Layers are perpendicular to the x_1-axis and their width is equal to ε' with $0 < r < 1$ In each layer fibers are cylinders of diameter ε and the orientation γ of which is a constant depending only on the layer (*see* Section 3 1)

In this model, a periodic homogenization is made in each layer (*see* Section 3 2) and then the layers are homogenized according to the rules of one dimensional media

In this model, the homogenized matrix $A^0(x)$ depends only on the matrix-valued function

$$\begin{pmatrix} 1 & 0 & 0 \\ 0 & -\sin\gamma(x_1) & \cos\gamma(x_1) \end{pmatrix} \tag{1 8}$$

where contrary to the first model, the variations of the orientation γ disappear

The third model exactly meets the requirements on the geometry we described at the beginning From the mathematical standpoint, this is the most interesting model because it involves a non-periodic homogenization problem which is not worked out by usual technics

More precisely, the fibrous material is composed here of layers perpendicular to the x_1-axis, the width of which is $s\varepsilon$ with $s > 1$ Each layer contains one rank of cylindrical fibers of diameter ε whose orientation only depends on the rank (*see* Section 4 1)

In this model, the homogenized matrix $A^0(x)$ depends on the matrix-valued function $\nabla\rho(x)$ defined by (1 7) but owing to the fibers cylindrical character, $A^0(x)$ satisfies the invariance condition (*see* Section 4 2)

$$\left.\begin{array}{l} x_1 = y_1 \\ d(x) = d(y) + 1 \end{array}\right\} \Rightarrow A^0(x) = A^0(y) \tag{1 9}$$

where the function $d(x)$ is defined in (1 7)

To perform the homogenization, the fibrous material is approximated by a « *locally periodic* » material which is periodic into cubes of size ε^r with $0 < r < 1$ (*see* Section 4.3). The locally periodic material is periodically homogenized by means of the usual homogenization formula (1.4) in each cube. Note that the scale ε^r does not appear naturally in this model as it does in the second model but it is only introduced « artificially » to obtain the homogenization result.

Finally the third model is compared to the first and second models (*see* Section 4.4).

This work is a survey of the two first parts of my thesis [Bri 1] and only the results are set out here. The mathematical details of the first and the second models are classical and those of the third model are in [Bri 2].

2. FIRST MODEL

2.1. Description

Let Ω be a bounded open set of $\mathbf{R}^3$.
Let χ be the characteristic function defined on $\mathbf{R}^2$ by

$$\begin{cases} \chi(y) = 1 & \text{if} \quad |y| \le 1/2 \\ \chi(y) = 0 & \text{if} \quad |y| > 1/2 \end{cases} \quad \text{and} \quad \chi \ Y\text{-periodic} \tag{2.1}$$

where $s > 1$ and $Y = [- s/2 \, ; s/2 \,]^2$.

The set $\{y \in \mathbf{R}^2 / \chi(y) = 1\}$ is a Y-periodic set of disks of diameter 1 as shown in figure 2 :

Let $\rho : \mathbf{R}^3 \to \mathbf{R}^2$ be the function defined by

$$\rho(x) = (x_1, \cos \gamma(x_1) x_3 - \sin \gamma(x_1) x_2) \quad \text{where} \quad \gamma \in C^1(\mathbf{R}). \tag{2.2}$$

Each connected part of the set $\{x \in \Omega / \chi(\rho(x)/\varepsilon) = 1\}$ is composed of straight lines of equation $\rho(x) = y = (y_1, y_2)$ where y belongs to a disk of diameter ε which implies $c_1 \le y_1 \le c_1 + \varepsilon$. Each straight line is contained between the planes $\{x_1 = c_1\}$ and $\{x_1 = c_1 + \varepsilon\}$ and makes an angle $\gamma(x_1)$ $(c_1 \le x_1 \le c_1 + \varepsilon)$ with the x_2-axis.

The matrix A^ε which characterizes the first model is defined by

$$A^\varepsilon(x) = A(\rho(x)/\varepsilon) \quad A = \chi A^1 + (1 - \chi) A^2 \tag{2.3}$$

where χ is the characteristic function defined by (2.1).

2.2. Homogenization result

The homogenization result for this type of problem is given without proof in [B.L.P.] Chap. 1 Section 18 (this model is called « stratified periodic homogenization » in this book). For a detailed proof of this result see [Bri 1].
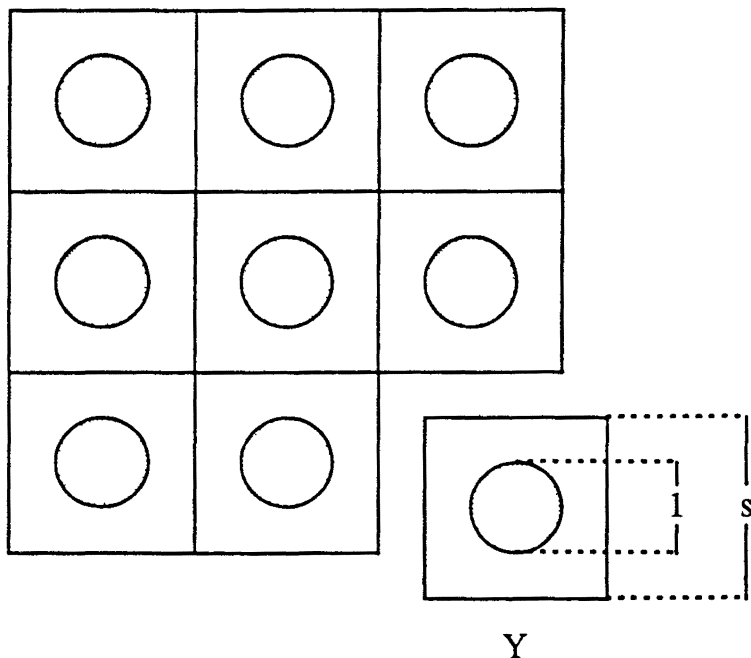
Y

Figure 2.

The homogenized matrix A^0 of the matrices A^ε defined by (2.3) is given by

$$A^0(x) \, \lambda \; = \; \frac{1}{|Y|} \int_Y [A(y) \, \lambda \; - A(y) \, {}^*\nabla\rho(x) \, \nabla_y\psi_\lambda(x, y)] \; dy \quad \forall \lambda \in \mathbf{R}^3 (2.4)$$

where the function $\psi_\lambda(x, y)$ is the unique solution (up to an additive constant) of the differential equation

$$\begin{cases} \mathrm{div}_y \, [\nabla\rho(x) A(y) \, {}^*\nabla\rho(x) \, \nabla_y\psi_\lambda(x, y)] = \mathrm{div}_y \, [\nabla\rho(x) A(y) \, \lambda] & \text{in } \mathbf{R}^2_y \\ \psi_\lambda(x, y) \; Y\text{-periodic of } y \end{cases}$$

$$(2.5)$$

(compare with formula (1.4)). In (2.5) x is a parameter, $\nabla\rho(x)$ is the derivative of function $\rho(x)$ defined by (2.2), i.e.

$$\nabla\rho(x) = \begin{pmatrix} 1 & 0 & 0 \\ -d(x) & -\sin\gamma(x_1) & \cos\gamma(x_1) \end{pmatrix} \qquad (2.6)$$

$$d(x) = \gamma'(x_1)[\cos\gamma(x_1)x_2 + \sin\gamma(x_1)x_3],$$

and ${}^*M$ denotes the transposed of the matrix M i.e. : ${}^*M_{ij} = M_{ji}$.

Remark 2.1 : The homogenized matrix-valued function A^0 is heteregeneous and depends only on the variable x_1. If the orientation γ of the fibers is constant, A^0 is also constant and this case corresponds to the periodic case described in the beginning of the Introduction.

2.3. Default of the model

Let us study the shape of a fiber in this model. To simplify the picture we only draw in figure 3 the square

$$c_1 \leqslant x_1 \leqslant c_1 + \varepsilon , \quad c_2 \leqslant [\cos \gamma (x_1) x_3 - \sin \gamma (x_1) x_2] \leqslant c_2 + \varepsilon .$$

Let us consider a fiber placed between the two planes $\{x_1 = c_1\}$ and $\{x_1 = c_1 + \varepsilon\}$ and suppose that function γ is not constant in a neighbourhood of c_1. Then the fiber is not cylindrical since extreme straight lines of the fiber make two different angles $\gamma (c_1)$ and $\gamma (c_1 + \varepsilon)$ with the x_2-axis as shown in figure 3.

The default in this model is due to the continuous variation of the function γ which deforms fibers, whereas the fibers orientation has to be constant in each fiber.

This problem is avoided in the following model which uses layers made of fibers with constant orientation.
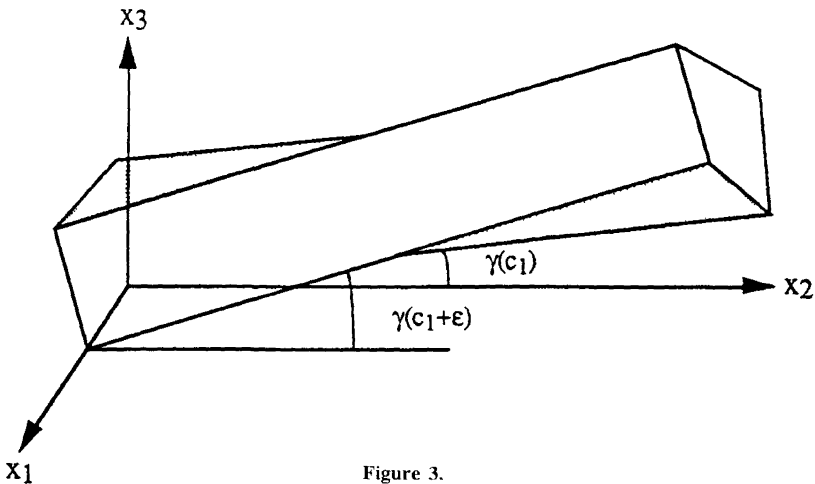

Figure 3.

3. SECOND MODEL

3.1. Description

The set Ω is divided in N_ε layers $\Omega_{\varepsilon, n}$ each of which is perpendicular to the x_1-axis and has a width ε^r with $r < 1$.

Let χ be the function defined by (2.1) and $\rho(z, x)$ the function defined by

$$\rho(z, x) = (x_1, \cos \gamma(z) x_3 - \sin \gamma(z) x_2) \quad \forall z \in \mathbf{R}, \quad \forall x \in \mathbf{R}^3 \quad (3.1)$$

where $\gamma \in C^1(\mathbf{R})$.

Let $x^{\varepsilon, n}$ be any point of $\Omega_{\varepsilon, n}$.

Behaviour law A^ε of layers material is defined by

$$A^\varepsilon(x) = A(\rho(x_1^{\varepsilon, n}, x)/\varepsilon) \quad \forall x \in \Omega_{\varepsilon, n} \quad (3.2)$$

where the matrix-valued function A is defined as in (2.3) by $A = \chi \ A^1 + (1 - \chi) A^2$.

In each layer $\Omega_{\varepsilon, n}$ of width ε^r, the fibrous material is defined as in the first model with the function $\rho(x_1^{\varepsilon, n}, x)$ which is parametrized by the point $x^{\varepsilon, n}$. But since the function $\rho(x_1^{\varepsilon, n}, x)$ is linear of x, this model actually describes a periodic set of fibers in the layer $\Omega_{\varepsilon, n}$: the fibers are cylinders of diameter ε and make a constant angle with the x_2-axis, equal to $\gamma(x_1^{\varepsilon, n})$ (see fig. 4).

Remark 3.1 : In this model which uses layers and a parametrization of the fibers orientation in each layer, cylindrical fibers are obtained the orientation of which changes in the fibrous material from layer to layer.

Each fiber has ε width while the layer has ε^r width. The number of fibers rank in each layer is thus proportional to ε^{r-1} and very large with respect to 1. This allows us to homogenize periodically in each layer according to the classical formula (1.4).

3.2. Homogenization result

Since the layers have ε^r width with $r < 1$, the fibrous material is « *locally periodic* » i.e. periodic in each layer and periodic homogenization can be performed from layer to layer. This « *locally periodic homogenization* » is based on the difference between fibers scale (ε) and layers scale (ε^r) (see e.g. [Bri 1] and [Bri 2] for locally periodic homogenization). The homogenized matrix A^0 of the matrices A^ε given by (3.2) is defined by

$$A^0(x) \lambda = \frac{1}{|Y|} \int_Y [A(y) \lambda - A(y) \, {}^*\nabla_x \rho(x_1, X) \, \nabla_y \psi_\lambda(x_1, y)] \, dy \quad \forall \lambda \in \mathbf{R}^3$$

$$(3.3)$$

where the function $\psi_\lambda(x_1, y)$ is the unique (up to an additive constant) solution of the differential equation

$$\begin{cases} \operatorname{div}_y [\nabla_x \rho(x_1, X) A(y) \, {}^*\nabla_x \rho(x_1, X) \, \nabla_y \psi_\lambda(x_1, y)] = \\ = \operatorname{div}_y [\nabla_x \rho(x_1, X) A(y) \lambda] \quad \text{in } \mathbf{R}_y^2 \quad \psi_\lambda(x_1, y) \; Y\text{-periodic of } y \end{cases} \quad (3.4)$$
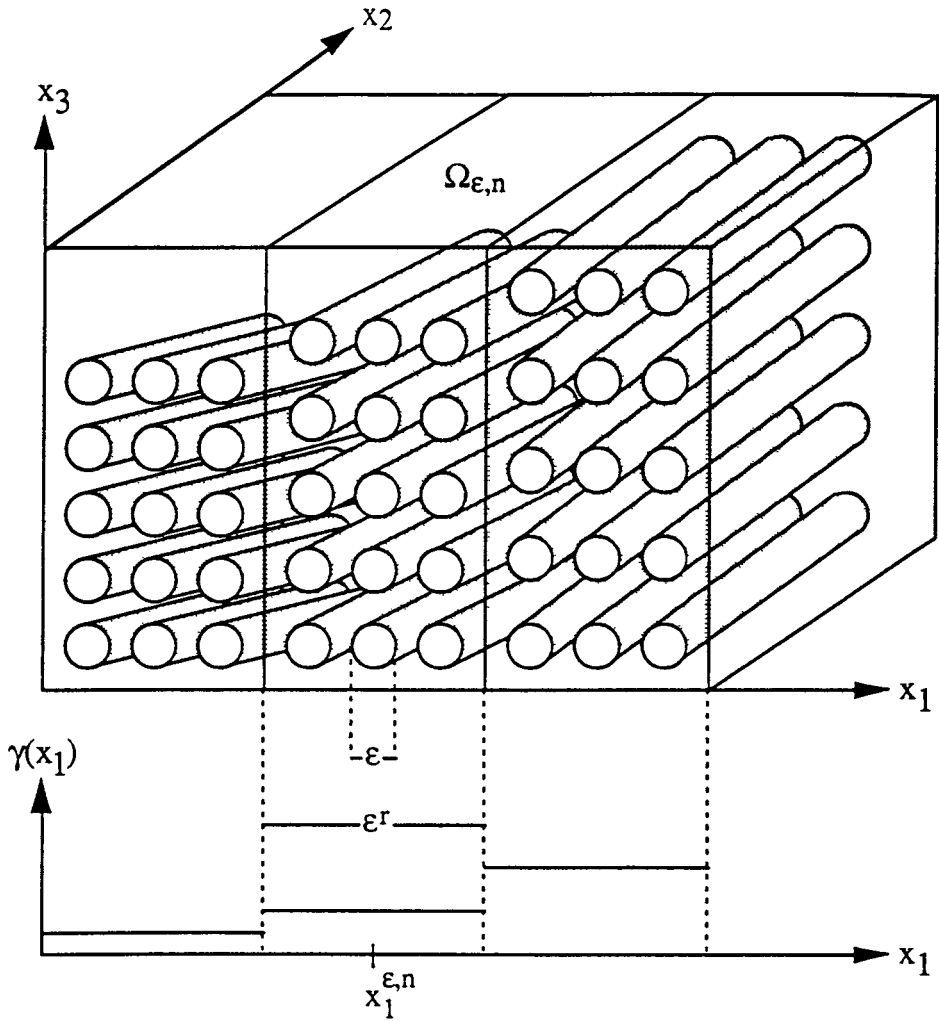
Figure 4

and $\nabla_x \rho(x_1, X)$ is the derivative with respect to x of the function $\rho(z, x)$ defined by (3 1) at the point $(z, x) = (x_1, X)$ i e

$$\nabla_x \rho(x_1, X) = \begin{pmatrix} 1 & 0 & 0 \\ 0 & -\sin\gamma(x_1) & \cos\gamma(x_1) \end{pmatrix} \qquad (3\ 5)$$

Note that $x_1 \in \mathbf{R}$ is a parameter in (3 4) while $X \in \mathbf{R}^3$ does not play any role in (3 4) since the function $\rho(z, x)$ is linear of x

Remark 3.2 : The homogenized matrix A^0 defined by (3.3) is heterogeneous but depends only on x_1 through the orientation function $\gamma(x_1)$.

3.3. Default of the model

By comparing the matrix-valued function $\nabla \rho(x)$ defined by (2.6) and the matrix-valued function $\nabla_x \rho(x_1, X)$ defined by (3.5), the second model appears to cancel the variations of the orientation function γ by taking it constant in each layer. But this is also the default of this model : there is discontinuity of the orientation between layers which are homogenized independently.
The third model where each layer is composed of one rank of fibers solves this difficulty.

4. THIRD MODEL

4.1. Description

This model consists of ranks of cyclindrical fibers perpendicular to the x_1-axis. In each rank the fibers are parallel and the fibers orientation changes from rank to rank (*see fig.* 4.1).
The x_1-coordinate of the ranks is given by $x_1 = k_1 \, s\varepsilon$ for $k_1 \in \mathbf{Z}$. Each layer of coordinate $x_1 = k_1 \, s\varepsilon$ is made of parallel cylindrical fibers of diameter ε perpendicular to the x_1-axis and make an angle $\gamma(k_1 \, s\varepsilon)$ with the x_2-axis. Each fiber is a cylinder $C_\varepsilon(k_1, k_2)$ of axis $\Delta_\varepsilon(k_1, k_2)$ parametrized by the pair $(k_1, k_2) \in \mathbf{Z}^2$ and defined by the parametric equation

$$
\left\{
\begin{array}{l}
C_\varepsilon(k_1, k_2) = \left\{ x \in \mathbf{R}^3 / \mathrm{dist}\,[x, \Delta_\varepsilon(k_1, k_2)] \leq \varepsilon \right\} \\[2mm]
\Delta_\varepsilon(k_1, k_2) = \left\{ x = \begin{pmatrix} x_1 \\ x_2 \\ x_3 \end{pmatrix} = \begin{pmatrix} k_1 \, s\varepsilon \\ t \cos \gamma(k_1 \, s\varepsilon) \\ k_2 \, s\varepsilon / \cos \gamma(k_1 \, s\varepsilon) + t \sin \gamma(k_1 \, s\varepsilon) \end{pmatrix} \middle| t \in \mathbf{R} \right\} \\[2mm]
\text{where} \quad s > 1 \quad \text{and} \quad \gamma \in C^2(\mathbf{R}) | \gamma | < \pi/2 .
\end{array}
\right.
$$

$$(4.1)$$

Between the two planes defined by $\{ x_1 = k_1 \, s\varepsilon - \varepsilon/2 \}$ and $\{ x_1 = k_1 \, s\varepsilon + \varepsilon/2 \}$ there is thus a rank of parallel cylindrical fibers of diameter ε which are perpendicular to the x_1-axis and make an angle $\gamma(k_1 \, s\varepsilon)$ with the x_2-axis. The distance between $\Delta_\varepsilon(k_1, k_2)$ and $\Delta_\varepsilon(k_1 + 1, k_2)$ or $\Delta_\varepsilon(k_1, k_2 + 1)$ is $s\varepsilon$.

Remark 4.1 : Contrary to the second model, this model is no more locally periodic since the variations of the fibers orientation are of the same order as

the fibers diameter. We will nevertheless see in Section 4.3 that this non-periodic material can be approximated by a « *locally periodic material* » which has to be locally periodically homogenized as the material of the second model.

The matrix A^ε of the fibrous material is defined by

$$
\begin{cases}
A^\varepsilon(x) = A^1 \Leftrightarrow x \in \bigcup_{(k_1, k_2) \in \mathbf{Z}^2} C_\varepsilon(k_1, k_2) \\[4mm]
A^\varepsilon(x) = A^2 \Leftrightarrow x \notin \bigcup_{(k_1, k_2) \in \mathbf{Z}^2} C_\varepsilon(k_1, k_2).
\end{cases}
\tag{4.2}
$$

4.2. Homogenization result

To state the homogenization result, we have to introduce a family of periodic materials parametrized by a point z of $\mathbf{R}^3$. Let $Y(z)$ be the parallelogram defined by

$$
Y(z) = \{t_1\, e_1(z) + t_2\, e_2/\, (t_1, t_2) \in [0\,;\,1]^2\} \quad \text{with} \quad
\begin{cases}
e_1(z) = \begin{pmatrix} s \\ s\, d(z) \end{pmatrix}, \\[3mm]
e_2 = \begin{pmatrix} 0 \\ s \end{pmatrix}
\end{cases}
\tag{4.3}
$$

$$
\text{where} \quad d(z) = \gamma'(z_1)[\cos \gamma(z_1)\, z_3 - \sin \gamma(z_1)\, z_3].
$$

Let $\chi(z, y)$ be the characteristic function defined by

$$
\chi(z, y) = \sum_{(k_1, k_2) \in \mathbf{Z}^2} \chi^0(y - k_1\, e_1(z) - k_2\, e_2)
\tag{4.4}
$$

where
$$
\begin{cases}
\chi^0(x) = 1 & |x| \leqslant 1/2 \\
\chi^0(x) = 0 & |x| > 1/2
\end{cases}
$$

which is $Y(z)$-periodic.

The set $\{y \in \mathbf{R}^2 / \chi(z, y) = 1\}$ is a $Y(z)$-periodic set of disks of diameter 1 as shown in figure 6.

Let B_z^ε be the matrix-valued function defined from the function $\chi(z, y)$ given by (4.4) through

$$
B_z^\varepsilon(x) = A(z, R(z_1)(x - z)/\varepsilon) \quad A(z, y) = \chi(z, y)\, A^1 + (1 - \chi(z, y))\, A^2
\tag{4.5}
$$

$$
\text{where} \quad R(z_1) = \begin{pmatrix} 1 & 0 & 0 \\ 0 & -\sin \gamma(z_1) & \cos \gamma(z_1) \end{pmatrix}.
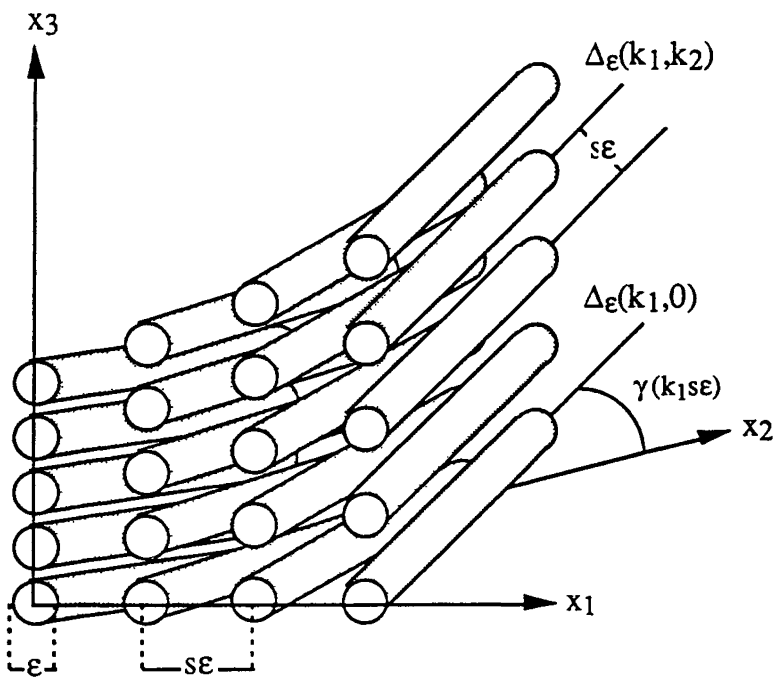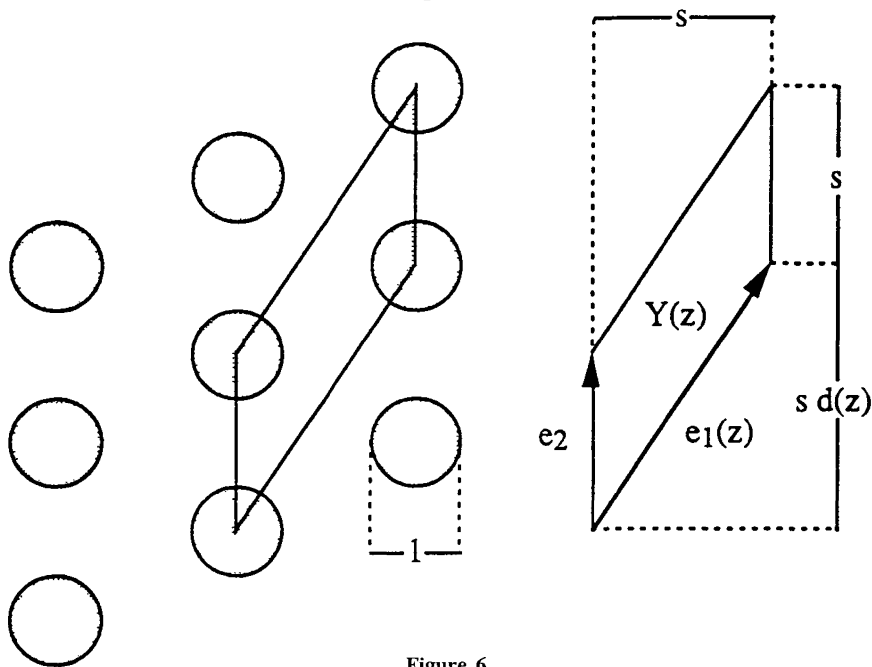$$

Figure 5.

Figure 6.

For z fixed, B_z^ε is the matrix of a periodic fibrous material as defined in the Introduction. This material is composed of parallel cylindrical fibers of diameter ε which are perpendicular to the x_1-axis, and make an angle $\gamma(z_1)$ with the x_2-axis. Note that by cutting this fibrous periodic material by the plane $\{x_2' = \cos \gamma(z_1) x_2 + \sin \gamma(z_1) x_3 = 0\}$, we obtain for $\varepsilon = 1$ the periodic set of disks of the figure 6 in the plane of the new coordinates (x_1', x_3') defined by

$$\begin{pmatrix} x_1' \\ x_3' \end{pmatrix} = R(z_1) x \quad \text{or} \quad \begin{cases} x_1' = x_1 \\ x_3' = \cos \gamma(z_1) x_3 - \sin \gamma(z_1) x_2 . \end{cases}$$

The homogenized matrix A^0 of the matrices A^ε defined by (4.2) is defined for each point x by $A^0(x) = B_x^0$, where B_x^0 is the homogenized matrix of the periodic matrices B_x^ε defined by (4.5). The classical homogenization formulas (1.4) and (1.5) for the periodic case thus give

$$A^0(x) \lambda = \frac{1}{|Y(x)|} \int_{Y(x)} [A(x, y) \lambda - A(x, y) *R(x_1) \nabla_y \psi_\lambda (x, y)] \, dy$$

$$\forall \lambda \in \mathbf{R}^3 \quad (4.6)$$

where the function $\psi_\lambda (x, y)$ is the unique solution (up to an additive constant) of the differential equation

$$\begin{cases} \operatorname{div}_y [R(x_1) A(x, y) *R(x_1) \nabla_y \psi_\lambda (x, y)] = \operatorname{div}_y [R(x_1) A(x, y) \lambda] & \text{in } \mathbf{R}_y^2 \\ \psi_\lambda (x, y) \, Y(x)\text{-periodic of } y \end{cases}$$

$$(4.7)$$

where the period $Y(x)$ is defined by (4.3) and the matrix-valued function $A(x, y)$ by (4.5). Here $x \in \mathbf{R}^3$ is only a parameter.

The matrix-valued function A^0 satisfies the invariance condition

$$\left. \begin{matrix} x_1 = y_1 \\ d(x) = d(y) + 1 \end{matrix} \right\} \Rightarrow A^0(x) = A^0(y)$$

where

$$d(x) = \gamma'(x_1)[\cos \gamma(x_1) x_2 + \sin \gamma(x_2) x_3] . \quad (4.8)$$

Remark 4.2 : The invariance condition (4.8) is easy to obtain mathematically. Indeed, when the x_1-coordinate is fixed, the periodic set of fibers which is associated to the matrix B_x^ε defined by (4.5), makes a fixed angle $\gamma(x_1)$ with the x_2-axis and is unchanged when we replace $d(x)$ by $d(x) + 1$ in the period $Y(x)$ as shown in figure 6. The matrices B_x^ε and their homogenized matrix $A^0(x)$ are thus unchanged and the condition (4.8) is proved.

The invariance condition (4.8) can be found geometrically as follows. For some fixed integer k_1, consider the axes $\Delta_\varepsilon(k_1, k_2)$ of the fibers $C_\varepsilon(k_1, k_2)$ defined by (4.1) and the projections on the plane $\{x_1 = k_1 s\varepsilon\}$ of the axes $\Delta_\varepsilon(k_1 + 1, k_2)$ of the fibers $C_\varepsilon(k_1 + 1, k_2)$. These projections intersect the axes $\Delta_\varepsilon(k_1, k_2)$ periodically with a period T_ε in the direction $x_2' = \cos \gamma(k_1 s\varepsilon) x_2 + \sin \gamma(k_1 s\varepsilon) x_3$ of the axes $\Delta_\varepsilon(k_1, k_2)$, as shown in figure 7.

This period T_ε is defined by

$$T_\varepsilon = \frac{s\varepsilon}{\tan \theta_\varepsilon} \quad \text{with} \quad \theta_\varepsilon = \gamma(k_1 s\varepsilon + s\varepsilon) - \gamma(k_1 s\varepsilon)$$

and satisfies $\qquad \lim_{\varepsilon \to 0} T_\varepsilon = \dfrac{1}{\gamma'(c_1)} \quad \text{if} \quad \lim_{\varepsilon \to 0} k_1 s\varepsilon = c_1 .$

When ε converges to 0, the period $1/\gamma'(c_1)$ then appears in the plane $\{x_1 = c_1\}$ along the direction $x_2' = \cos \gamma(c_1) x_2 + \sin \gamma(c_1) x_3$. When the x_1-coordinate is fixed, the homogenized matrix $A^0(x)$ is thus periodic with the period $1/\gamma'(x_1)$ of the variable $\cos \gamma(x_1) x_2 + \sin \gamma(x_1) x_3$, which implies the condition (4.8).
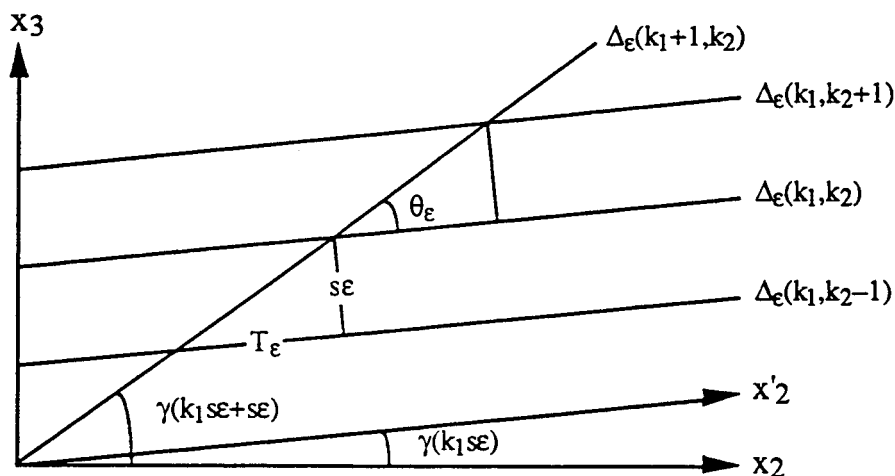

Figure 7.

4.3. Sketch of the proof of the homogenization result

We just give here an idea of the method used to homogenize non-periodic matrices A^ε defined by (4.2). Detailed proof is given in [Bri 1].

Let us first see how the shift function $d(z)$ which defines period $Y(z)$ in (4.3), appears :

Let x^ε be a point of the axis $\Delta_\varepsilon (k_1, k_2)$ defined in (4.1) and y^ε be the point of the axis $\Delta_\varepsilon (k_1 + 1, k_2)$ with the same x_2-coordinate than x^ε

$$x^\varepsilon = \begin{pmatrix} k_1 \, s\varepsilon \\ t \cos \gamma \, (k_1 \, s\varepsilon) \\ k_2 \, s\varepsilon/\cos \gamma \, (k_1 \, s\varepsilon) + t \sin \gamma \, (k_1 \, s\varepsilon) \end{pmatrix}$$

$$y^\varepsilon = \begin{pmatrix} k_1 \, s\varepsilon + s\varepsilon \\ t \cos \gamma \, (k_1 \, s\varepsilon) \\ k_2 \, s\varepsilon/\cos \gamma \, (k_1 \, s\varepsilon + s\varepsilon) + t' \sin \gamma \, (k_1 \, s\varepsilon + s\varepsilon) \end{pmatrix}.$$

The shift δ_ε along the x_3-axis between the points y^t and x^t is equal to (*see* fig. 8)

$$\delta_\varepsilon = y_3^\varepsilon - x_3^\varepsilon = b_3^\varepsilon - a_3^\varepsilon + x_2^\varepsilon \tan \gamma \, (x_1^\varepsilon + s\varepsilon) - x_2^\varepsilon \tan \gamma \, (x_1^\varepsilon)$$

$$= \frac{k_2 \, s\varepsilon}{\cos \gamma \, (x_1^\varepsilon + s\varepsilon)} - \frac{k_2 \, s\varepsilon}{\cos \gamma \, (x_1^\varepsilon)} + x_2^\varepsilon \tan \gamma \, (x_1^\varepsilon + s\varepsilon) - x_2^\varepsilon \tan \gamma \, (x_1^\varepsilon)$$

and by developing the previous term at order 1 in $s\varepsilon$, one obtains

$$\delta_\varepsilon = \frac{s\varepsilon \, d(x^\varepsilon)}{\cos \gamma \, (x_1^\varepsilon)} + O(\varepsilon^2).$$
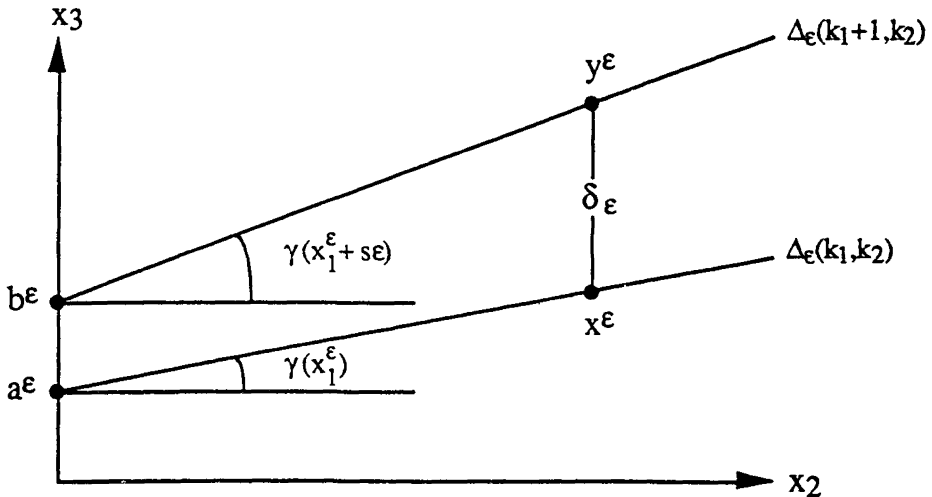

Figure 8.

The shift δ_ε is hence locally approximated by the shift $s\varepsilon \, d(x^\varepsilon)$ made in the direction $\cos \gamma \, (k_1 \, s\varepsilon) \, x_2 + \sin \gamma \, (k_1 \, s\varepsilon) \, x_3$ of the axis $\Delta_\varepsilon (k_1, k_2)$ in the plane $\{x_1 = x_1^\varepsilon\}$.

This local shift $s\varepsilon\, d(x^\varepsilon)$ will allow us to define a locally periodic fibrous material which approximates the non-periodic material A^ε defined by (4.2). This material is periodic in the neighbourhood of different points x^ε defined as follows :

The domain Ω is divided in N_ε cubes $Q_{\varepsilon,n}$ of size ε^r with $r < 1$. In each cube $Q_{\varepsilon,n}$, we fix a point $x^\varepsilon = x^{\varepsilon,n}$ and consider the matrix B_z^ε defined by (4.5), for the point $z = x^{\varepsilon,n}$. This matrix $B_{x^{\varepsilon,n}}^\varepsilon$ is associated to a periodic set of fibers whose shift is $s\varepsilon\, d(x^{\varepsilon,n})$.

The matrices A^ε defined by (4.2) are then compared to the locally periodic matrices B^ε defined by

$$B^\varepsilon(x) = B_{x^{\varepsilon,n}}^\varepsilon(x) \quad x \in Q_{\varepsilon,n}\,. \tag{4.9}$$

By a simple computation, one obtains the estimate

$$\int_\Omega |A^\varepsilon(x) - B^\varepsilon(x)|\, dx \leqslant c\varepsilon^{2r-1}\,. \tag{4.10}$$

Then by using an estimate of the difference between two homogenized limits (see [Don]) and by taking $r > 1/2$, estimate (4.10) implies the equality between homogenized matrices A^0 and B^0. On the other hand, the homogenized matrix B^0 is deduced from a locally periodic homogenization (see [Bri 2]) as in the second model. The homogenized matrix A^0 is hence given by formulas (4.6) and (4.7).

4.4. Comparison with the two previous models

Contrary to the second model but like in the first model, the third model depends on the variations of the orientation function γ.

The difference between the first model and the third model comes from the cylindrical character of the fibers in the first model. This difference appears in homogenization formulas (2.4) and (4.6) which respectively concern the first and third models. Indeed, after the linear change of variables defined by

$$y' = D(x)\,y \quad \begin{cases} y \in Y(x) \\ y' \in Y \end{cases} \quad \text{where} \quad D(x) = \begin{pmatrix} 1 & 0 \\ -d(x) & 1 \end{pmatrix}$$

the homogenization formula (4.6) of the third model becomes

$$A^0(x)\,\lambda = \frac{1}{|Y|} \int_Y [A'(x, y')\,\lambda - A'(x, y') * (D(x)\,R(x_1))\,\nabla_{y'}\chi_\lambda(x, y')]\, dy'$$

$$\forall \lambda \in \mathbf{R}^3 \quad (4.11)$$

where the matrix-valued function $D(x)\,R(x_1)$ is equal to the function $\nabla\rho(x)$ defined by (2.6). The difference between the homogenization formula

(4.11) of the third model and the formula (2.4) of the first one comes from the difference between the function $A'(x, y')$ which depends on x in formula (4.11) and the function $A(y)$ which does not in formula (2.4). In some sense, the function $A'(x, y')$ in the third model « regularizes » the deformation due to the function $\rho(x)$ in the first model.

REFERENCES

[Art] M. J. ARTS, 1978, *A Mathematical Model of the Dynamics of the Left Ventricle,* Thesis, University of Limburg, The Netherlands.

[B.L.P.] A. BENSOUSSAN, J. L. LIONS, G. PAPANICOLAOU, 1978, *Asymptotic Analysis for Periodic Structures,* North-Holland, Amsterdam.

[Bri 1] M. BRIANE, 1990, Homogénéisation de matériaux fibrés et multi-couches, Thèse de l'Université Paris 6.

[Bri 2] M. BRIANE, Homogenization of a non-periodic material, *Math. Pures Appl.,* to appear.

[Cha] R. S. CHADWICK, 1982, Mechanics of the left ventricle, *Biophys. J.,* 39, 279-288.

[Don] P. DONATO, 1983, Una stima per la differenza di H-limiti e qualche applicazione a problemi di omogeneizzazione, *Rendiconti di Matematica,* 4, Vol. 3, Serie VII.

[Feit] T. S. FEIT, 1979, Diastolic pressure-volume relations and distribution of pressure and fiber extension across the wall of model left ventricle, *Biophys. J.,* 28, 143-166.

[Mur] F. MURAT, 1978, *H-Convergence,* Séminaire d'Analyse Fonctionnelle et Numérique, University of Algiers, Multigraphed.

[Pes] C. S. PESKIN, 1989, Fiber architecture of the left ventricular wall : an asymptotic analysis, *Comm. Pure and Appl. Math.,* 42, 79-113.

[San] E. SANCHEZ-PALENCIA, 1980, Non Homogeneous Materials and Vibration Theory, Springer Verlag, Monographs in Physics, V. 127, Berlin.

[Spa] S. SPAGNOLO, 1968, Sulla convergenza di soluzioni di equazioni paraboliche e ellitiche, *Ann. Sc. Norm. Sup. Pisa,* 22, 571-597.

[Str] D. D. STREETER, 1979, Gross Morphology and Fiber Geometry of the Heart, *Handbook of Physiology,* Vol. 1, Section 2, American Physiology Society, Bethesda, Maryland.

[Tar] L. TARTAR, 1977, *Cours Peccot au Collège de France,* unpublished.